Bonding Properties of the 1,2-Semiquinone Radical-Anionic Ligand in the $[M(CO)_{4-n}(L)_n(DBSQ)]$ Complexes (M = Re, Mn; DBSQ = 3,5-di-*tert*-butyl-1,2-benzosemiquinone; *n* = 0, 1, 2). A Comprehensive Spectroscopic (UV−Vis and IR Absorption, Resonance Raman, EPR) and Electrochemical Study

František Hartl*,† and Antonín Vlček, Jr.*,‡

Anorganisch Chemisch Laboratorium, J. H. van't Hoff Instituut, Universiteit van Amsterdam, Nieuwe Achtergracht 166, NL-1018 WV Amsterdam, The Netherlands, and J. Heyrovský Institute of Physical Chemistry, Academy of Sciences of the Czech Republic, Dolejškova 3, 182 23 Prague, Czech Republic

Received January 10, 1995[⊗]

Rhenium and manganese complexes of the 3,5-di-*tert*-butyl-1,2-benzosemiquinone (DBSQ) ligand, $[M(CO)_4(DBSQ)]$, *fac*-$[M(CO)_3(L)(DBSQ)]$, and *cis,trans*-$[M(CO)_2(L)_2(DBSQ)]$, with a widely varied nature of co-ligand(s) (L = THF, Me_2CO, MeC(O)Ph, py, NEt_3, Ph_3PO, $SbPh_3$, $AsPh_3$, PCy_3, $P(OPh)_3$, PPh_3, dppe-*p*, PPh_2Et, $P(OEt)_3$, PEt_3) were generated in solution and characterized as valence-localized molecules containing the radical-anionic DBSQ ligand bound to Re^I or Mn^I metal atoms. This is evidenced by the following. (i) Carbonyl stretching frequencies ν(C≡O) and average force constants k_{av} are typical for Mn^I or Re^I carbonyls. (ii) Frequencies of the intra-dioxolene C═O bond stretching vibration, ν(C═O), lie within the 1400−1450 cm^{-1} range which is diagnostic for coordinated semiquinones. (iii) EPR spectra indicate a very small spin density on the metal atom ($0.2\% < a_M/A_{iso} > 2.6\%$). (iv) Absorption spectra show $Re^I \rightarrow$ DBSQ MLCT electronic transitions characterized by a resonant enhancement of the Raman peaks due to the ν(C≡O) and intra-DBSQ ν(C═O) vibrations. (iv) Finally, the electrochemical pattern consists of DBSQ/DBQ and DBSQ/DBCat ligand-localized redox couples. All these properties are, in a limited range, dependent on the nature and, especially, the number of co-ligands L, indicating a small delocalization of the singly occupied MO of the DBSQ ligand over the metal atom. The extent of this delocalization may be finely tuned by changing the co-ligands, although in absolute terms, it remains rather limited, and the DBSQ ligand behaves toward Re^I and Mn^I as a very weak π-acceptor only. The changes of the electronic properties of the metal center induced by the co-ligands are mostly compensated by more flexible M $\rightarrow$ CO π back-bonding as is manifested by large variations of the average C≡O stretching force constant.

Introduction

o-Semiquinone radical-anions[1] are very remarkable ligands, able to form stable radical complexes with both transition[2,3] and nontransition[4,5] metals. When bound to a metal atom that does not possess unpaired electrons and that is difficult both to reduce and to oxidize, semiquinones (SQ) often behave as organic radicals stabilized by the coordination. Some SQ complexes of Co^{III} [6−9] or of nontransition metals like Zn^{II} [10] are typical examples. Such complexes pose a unique opportunity to investigate the properties of a radical-anionic ligand and to study how the unpaired electron on the ligand interacts with the metal, thus affecting the behavior of the complex molecule. Semiquinones are redox-active ligands, see Scheme 1, which may easily be reduced to catecholates (Cat) and oxidized to quinones[1] (Q) while remaining bound to the metal.[2,3,11] Therefore, an ambiguity in the assignment of the oxidation states to the metal atom and to the dioxolene[1] ligand arises whenever a semiquinone is coordinated to a redox-active metal.[2,3,11] Thus, a complex molecule that contains a $[M^{n+}(SQ)]$ unit may, in principle, have two other valence isomers,[11] which differ only in the distribution of the electrons between the metal and the dioxolene ligand, $[M^{(n+1)+}(Cat)]$ and $[M^{(n-1)+}(Q)]$. Some dioxolene complexes are known to exist in two such different valence forms, depending on factors such as the nature of the co-ligands, environment, or temperature.[2,3,11] For example, copper−dioxolene complexes occur as Cu^I−semiquinone, $[Cu^I(L)_2(DBSQ)]$, when "soft" co-ligands such as phosphines, phosphites, CO, isonitriles, alkynes, alkenes, and thioethers are pres-

Scheme 1

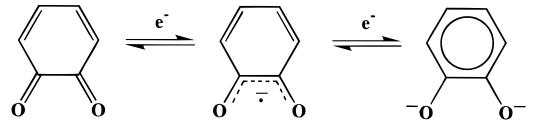

† Universiteit van Amsterdam.
‡ J. Heyrovský Institute.
⊗ Abstract published in *Advance ACS Abstracts,* January 15, 1996.

(1) The term "dioxolene" (Diox) is used for ligands derived from 1,2-dioxobenzene, irrespective of their oxidation state, i.e. for catecholate dianion (Cat), *o*-semiquinone radical-anion (SQ), or *o*-quinone (Q), without specifying the substituents on the benzene ring. The individual oxidation states of the 3,5-di-*tert*-butyl-1,2-dioxobenzene (DBDiox) are denoted DBCat, DBSQ, and DBQ.

(2) Pierpont, C. G.; Buchanan, R. M. *Coord. Chem. Rev.* **1981**, *38*, 45.
(3) Pierpont, C. G.; Lange, C. W. *Prog. Inorg. Chem.* **1994**, *41*, 331.
(4) Felix, C. C.; Sealy, R. C. *J. Am. Chem. Soc.* **1982**, *104*, 1555.
(5) Tuck, D. G. *Coord. Chem. Rev.* **1992**, *112*, 215.
(6) Wicklund, P. A.; Beckmann, L. S.; Brown, D. G. *Inorg. Chem.* **1976**, *15*, 1996.
(7) Kessel, S. L.; Emberson, R. M.; Debrunner, P. G.; Hendrickson, D. N. *Inorg. Chem.* **1980**, *19*, 1170.
(8) Hartl, F.; Vlček, A., Jr. *Inorg. Chim. Acta* **1986**, *118*, 57.
(9) Benelli, C.; Dei, A.; Gatteschi, D.; Pardi, L. *Inorg. Chim. Acta* **1989**, *163*, 99.
(10) Benelli, C.; Dei, A.; Gatteschi, D.; Pardi, L. *Inorg. Chem.* **1989**, *28*, 1476.
(11) Vlček, A., Jr. *Comments Inorg. Chem.* **1994**, *16*, 207.

0020-1669/96/1335-1257$12.00/0

ent in their coordination spheres.[12−15] When the ligand L is substituted for a harder ligand, *e.g.*, 2,2′-bipyridine, a complete switchover to the [Cu^{II}(bpy)(DBCat)] isomer occurs.[12−15] Subtle co-ligand control of the electron distribution within the [M(Diox)] unit was found also for [$Co^{II}(L_2)(DBSQ)_2$]/[$Co^{III}(L_2)$(DBCat)-(DBSQ)] or [$Mn^{II}(L_2)(DBSQ)_2$]/[$Mn^{III}(L_2)$(DBCat)(DBSQ)]/[$Mn^{IV}(L_2)(DBCat)_2$] groups of bistable complexes[16−18] and for some dioxolene complexes of Mn, Rh, etc.[2,3,11] Such switching of the electron localization between two sharply defined valence forms, induced by a co-ligand change, indicates very little electronic delocalization within the metal−dioxolene chelate rings [M(SQ)] and [M(Cat)]. However, although most semiquinone complexes appear to be valence-localized[11] with well-defined metal and ligand (*i.e.* SQ) oxidation states, an occurrence of a delocalized structure $[M(Diox)]^{n+}$ cannot be a *priori* excluded.

Mixed-ligand carbonyl−semiquinone complexes of Re and Mn, [$M(CO)_{4-n}(L)_n$(DBSQ)] (n = 0, 1, 2) are very suitable systems to investigate the co-ligand influence on the electron distribution and (de)localization between the metal and the semiquinone ligand. Although the radical character of these complexes was recognized earlier,[19−31] no such systematic study has been undertaken so far. Hence, to better understand the bonding properties of the DBSQ ligand, we have generated a series of complexes [$M(CO)_{4-n}(L)_n$(DBSQ)] (M = Re, Mn; n = 0, 1, 2) (see Figure 1) with the co-ligands L of widely varied bonding properties and studied their IR, resonance Raman, electronic absorption, and EPR spectra, as well as the electrochemical redox potentials. When the information obtained was combined, it was possible to address the question of how increasing electron density on the metal atom influences the extent of electronic delocalization within the [M^I(SQ)] chelate ring.

Experimental Section

Materials. 3,5-Di-*tert*-butyl-1,2-benzoquinone, DBQ (Aldrich), was recrystallized from *n*-heptane. $Re_2(CO)_{10}$ and $Mn_2(CO)_{10}$ (Strem) were used without further purification. Purity of the ligands (L = THF, Me_2CO, MeC(O)Ph, py, NEt_3, Ph_3PO, $SbPh_3$, $AsPh_3$, PCy_3, $P(OPh)_3$, PPh_3, dppe-*p*, PPh_2Et, $P(OEt)_3$, PEt_3 obtained commercially (Fluka, Aldrich, BDH, Merck)] was checked by melting points and by NMR. If necessary, they were purified by recrystallization or distillation under reduced pressure. Bu_4NPF_6 (Fluka) was dried *in vacuo* at 80 °C for 10 h. $[Cp_2Fe]BF_4$ was synthesized by a published method.[32] [Bu_4N][$Mn(CO)_3$(DBCat)] was prepared according to ref 33. Solvents (spectroscopic grade) were freshly distilled under argon or nitrogen atmosphere. THF and CH_2Cl_2 (Fluka) were distilled from a sodium−benzophenone mixture or from P_2O_5, respectively. Pyridine (Merck) was dried by refluxing with KOH followed by a fractional distillation. Benzene was distilled from a Na wire or from $LiAlH_4$. Solutions for photolyses were freeze−pump−thaw degassed and handled under vacuum. Electrochemical and spectroscopic studies were carried out using argon or nitrogen atmosphere.

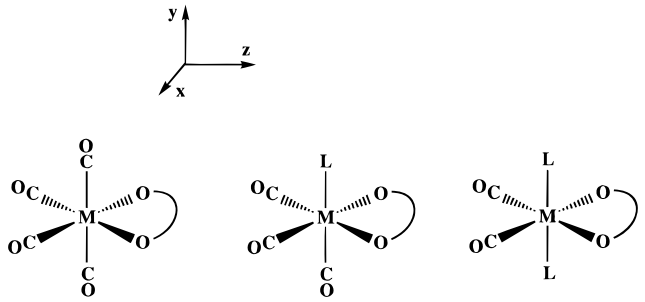

Figure 1. Structures of the [$M(CO)_{4-n}(L)_n$(DBSQ] complexes (M = Re or Mn, n = 0, 1, 2). M = Re: n = 0, 1, L = THF, Me_2CO, MeC(O)Ph, py, NEt_3, Ph_3PO, $SbPh_3$, $AsPh_3$, $P(OPh)_3$, PPh_3, dppe-*p*, PPh_2Et, PCy_3; n = 2, L = PPh_3, $P(OPh)_3$, $AsPh_3$. M = Mn: n = 0, 1, L = THF, CH_3CN, PPh_3, py, H_2O; n = 2, L = $P(OPh)_3$, $P(OEt)_3$, PPh_3, PEt_3.

Generation of Semiquinone Complexes. [$Re(CO)_4$(DBSQ)] was generated by irradiation of a stirred solution (10 mL) of 5×10^{-3} M $Re_2(CO)_{10}$ and 10^{-2} M DBQ in degassed benzene or CH_2Cl_2 with a 125 W medium-pressure or a 200 W high-pressure mercury lamp overnight. The 300−370 nm irradiation spectral region was selected by a combination of the Pyrex glass of the reaction vessel and a UG11 Oriel band-pass filter. Nearly complete (>95%) conversion to [$Re(CO)_4$(DBSQ)] was accomplished, as was determined by IR spectra. [$Re(CO)_3$(L)(DBSQ)] complexes were generated by an addition of a 10-fold molar excess of the ligand L to the solutions of [$Re(CO)_4$-(DBSQ)] under vacuum or inert atmosphere. [$Re(CO)_2(L)_2$(DBSQ)] complexes, L = PPh_3, $P(OPh)_3$, or $AsPh_3$, were produced by photolysis of [$Re(CO)_3$(L)(DBSQ)] solutions with a 10-fold excess of L overnight.

[$Mn(CO)_3$(THF)(DBSQ)] was generated by an oxidation[28] of degassed THF solutions of [Bu_4N][$Mn(CO)_3$(DBCat)] with solid [Cp_2-Fe]BF_4. Subsequent addition of an excess of L = phosphines or phosphites to the solutions of [$Mn(CO)_3$(THF)(DBSQ)] cleanly formed [$Mn(CO)_2(L)_2$(DBSQ)] complexes while the reaction with pyridine led to [$Mn(CO)_3$(py)(DBSQ)]. [$Mn(CO)_3(PPh_3)$(DBSQ)] was prepared according to ref 31. The [$Mn(CO)_4$(DBSQ)] complex was produced by an oxidation of the CH_2Cl_2 solution [Bu_4N][$Mn(CO)_3$(DBCat)] with a small excess of $[Cp_2Fe]BF_4$ under CO atmosphere. Alternatively, the manganese−semiquinone complexes were generated by electrochemical oxidation of THF or CH_2Cl_2 solutions of [Bu_4N][$Mn(CO)_3$-(DBCat)] and the ligand L on a Pt-mesh electrode within a multipurpose optically transparent thin layer electrochemical (OTTLE) cell,[34] and their spectroscopic properties were studied *in situ*. [$Mn(CO)_2(PPh_3)_2$-(DBSQ)] was also produced by mixing [Bu_4N][$Mn(CO)_3$(DBCat)] with 2 equiv of PPh_3 and 1 equiv of $[Mn(CO)_2(PPh_3)_2(DBQ)](PF_6)$[31] in THF or CH_2Cl_2 solutions.

Instrumentation. Electronic absorption spectra were obtained on a Hewlett-Packard 8452A diode array or a Perkin-Elmer Lambda 5 spectrophotometer. Varian E4 and Bruker 300 X-band spectrometers were used to measure the EPR spectra. The *g* factors were determined against the DPPH standard (g = 2.0037). IR spectra were obtained

(12) Razuvaev, G. A.; Cherkasov, V. K.; Abakumov, G. A. *J. Organomet. Chem.* **1978**, *160*, 361.
(13) Buchanan, R. M.; Wilson-Blumenberg, C.; Trapp, C.; Larsen, S. K.; Greene, D. L.; Pierpont, C. G. *Inorg. Chem.* **1986**, *25*, 3070.
(14) Speier, G.; Tisza, S.; Tyeklár, Z.; Lange, C. W.; Pierpont, C. G. *Inorg. Chem.* **1994**, *33*, 2041.
(15) Rall, J.; Kaim, W. *J. Chem. Soc., Faraday Trans.* **1994**, *90*, 2905.
(16) Attia, A. S.; Pierpont, C. G. *Inorg. Chem.* **1995**, *34*, 1172.
(17) Adams, D. M.; Dei, A.; Rheingold, A. L.; Hendrickson, D. N. *J. Am. Chem. Soc.* **1993**, *115*, 8221.
(18) Jung, O.-S.; Pierpont, C. G. *Inorg. Chem.* **1994**, *33*, 2227.
(19) Creber, K. A. M.; Wan, J. K. S. *J. Am. Chem. Soc.* **1981**, *103*, 2101.
(20) Abakumov, G. A.; Cherkasov, V. K.; Shalnova, K. G.; Teplova, I. A.; Razuvaev, G. A. *J. Organomet. Chem.* **1982**, *236*, 333.
(21) Creber, K. A. M.; Ho, T.-I.; Depew, M. C.; Weir, D.; Wan, J. K. S. *Can. J. Chem.* **1982**, *60*, 1504.
(22) Creber, K. A. M.; Wan, J. K. S. *Chem. Phys. Lett.* **1981**, *81*, 453.
(23) van der Graaf, T.; Stufkens, D. J.; Víchová, J.; Vlček, A., Jr. *J. Organomet. Chem.* **1991**, *401*, 305.
(24) Creber, K. A. M.; Wan, J. K. S. *Can. J. Chem.* **1983**, *61*, 1017.
(25) Wang, S. R.; Cheng, C. P. *J. Chem. Soc., Dalton Trans.* **1988**, 2695.
(26) Ho, T.-I.; Chang, C.-M.; Wang, S. R.; Cheng, C. P. *J. Chem. Soc.* **1988**, 123.
(27) Hartl, F.; Vlček, A., Jr.; Stufkens, D. J. *Inorg. Chim. Acta* **1992**, *192*, 25.
(28) Hartl, F.; Vlček, A., Jr. *Inorg. Chem.* **1991**, *30*, 3048.
(29) Hartl, F.; Stufkens, D. J.; Vlček, A., Jr. *Inorg. Chem.* **1992**, *31*, 1687.
(30) Hartl, F.; Vlček, A., Jr. *Inorg. Chem.* **1992**, *31*, 2869.
(31) Hartl, F. *Inorg. Chim. Acta* **1995**, *232*, 99.
(32) Hendrickson, D. N.; Sohn, Y. S.; Gray, H. B. *Inorg. Chem.* **1971**, *10*, 1559.
(33) Hartl, F.; Vlček, A., Jr.; de Learie, L. A.; Pierpont, C. G. *Inorg. Chem.* **1990**, *29*, 1073.
(34) (a) Krejčík, M.; Daněk, M.; Hartl, F. *J. Electroanal. Chem. Interfacial Electrochem.* **1991**, *317*, 179. (b) Hartl, F.; Luyten, H.; Nieuwenhuis, H. A.; Schoemaker, G. C. *Appl. Spectr.* **1994**, *48*, 1522.

on the following FTIR instruments, detectors and spectral resolutions being specified in parentheses: Philips PU9800 (DTGS, 4 cm^{-1}), Nicolet 7199B (liquid N_2 cooled MCT, 1 cm^{-1}), and Bio-Rad FTS-7 (DTGS, 2 cm^{-1}). Resonance Raman spectra were measured on a Dilor XY Raman spectrometer that employs a backscattering geometry. Sample solutions were placed in demountable IR cells equipped with NaCl windows and excited either by a SP 2016 Ar^+ laser or by a CR-590 dye laser employing Coumarine 6 or Rhodamine 6G dyes pumped by the Ar^+ laser. Cyclic voltammetry measurements were performed in 10^{-3} M sample solutions containing 10^{-1} M Bu_4NPF_6 using a PA4 polarographic analyzer (EKOM, Czech Republic) or PAR Model 173 potentiostat. Potentials were measured on a Pt disk working electrode against a Ag wire pseudoreference electrode and are referenced to the ferrocene/ferrocenium (Fc/Fc^+) redox couple used as an internal standard.[35] Spectroelectrochemical generation and investigation of the Mn−semiquinone complexes were carried out in an IR-OTTLE cell[34] equipped with a Pt minigrid working electrode (6 × 5 mm rectangle, 32 wires/cm). The same OTTLE cell[34] was used to obtain Raman, FTIR, and UV−vis absorption spectra using NaCl, KBr, and CaF_2 windows, respectively. Usual sample concentrations for the spectroelectrochemical studies were in the range 5×10^{-3} to 10^{-2} M with 3×10^{-1} M Bu_4NPF_6 added.

Results and Discussion

The complexes studied were characterized in solution by their FTIR and EPR spectra which confirmed their compositions and structures shown in Figure 1. No radical- or carbonyl-containing impurities have been detected.

IR Spectra in the *ν*(C≡O) Region. IR *ν*(C≡O) stretching frequencies of the complexes under study are summarized in Table 1. Typical[36−39] spectral patterns observed are consistent with the configurations indicated in Figure 1, *i.e*. *cis*-[$M(CO)_4$(DBSQ)], *fac*-[$M(CO)_3$(DBSQ)], and *cis*,*trans*-[$M(CO)_2(L)_2$(DBSQ)] with the two ligands in the axial positions. Individual C≡O stretching force constants were not obtained as no unequivocal assignment of the IR bands of the tetra- and tricarbonyls is possible[36−39] without the isotopic substitution. Instead, an average force constant,[37] k_{av}, has been calculated (Table 1) and used as an indication of the extent of the M → CO π-back-donation. The k_{av} values decrease rapidly with decreasing number of CO ligands present in the coordination sphere. For the substituted species, k_{av} decreases in the order L = $P(OPh)_3$ > $P(OMe)_3$ > PPh_3 > PPh_2Et > PR_3, *i.e*. with decreasing π-acceptor and increasing σ-donor capacity of the phosphorus ligand. Among the tricarbonyls, the lowest k_{av} values were found for hard σ-donors without any prominent π-bonding properties: L = THF, MeC(O)Ph, NEt_3, py, Me_2CO, and Ph_3PO.

EPR Spectra. All the semiquinone complexes investigated exhibit intense EPR signals (see Table 2 for parameters) centered at *g* values that are only slightly lower than the *g* factor of the free DBSQ radical-anion ($g = 2.0051$ in 10^{-1} M Bu_4NPF_6/THF),[23] indicating that the unpaired electron is dominantly localized on the DBSQ radical ligand. Small, but definite, deviation of the g-factors below the free DBSQ value points to the presence of a low-lying unoccupied MO that is mixed with the singly occupied MO (SOMO), both MO's involved containing small contributions from the metal d orbitals.[40,41]

Table 1. Infrared C≡O Stretching Frequencies of the Re and Mn Carbonyl−Semiquinone Complexes[a]

complex	solvent	*ν*(C≡O) IR bands, cm^{-1}	k_{av}, N m^{-1}
[$Re(CO)_4$(DBSQ)]	C_6H_6	2109, 2010, 1987, 1942	1636
[$Re(CO)_4$(DBSQ)]	CH_2Cl_2	2110, 2011, 1985, 1938	1635
[$Re(CO)_3(P(OPh)_3)$(DBSQ)]	C_6H_6	2037, 1959, 1916	1569
[$Re(CO)_3(P(OPh)_3)$(DBSQ)]	CH_2Cl_2	2036, 1950, 1910	1560
[$Re(CO)_3(SbPh_3)$(DBSQ)]	C_6H_6	2022, 1931, 1907	1542
[$Re(CO)_3(AsPh_3)$(DBSQ)]	C_6H_6	2022, 1931, 1904	1540
[$Re(CO)_3(AsPh_3)$(DBSQ)]	CH_2Cl_2	2021, 1926, 1899	1535
[$Re(CO)_3(PPh_3)$(DBSQ)]	C_6H_6	2022, 1932, 1902	1540
[$Re(CO)_3(PPh_3)$(DBSQ)]	CH_2Cl_2	2020, 1928, 1896	1534
[$Re(CO)_3(PPh_3)$(DBSQ)]	THF	2020, 1928, 1902	1537
[$Re(CO)_3(PPh_2Et)$(DBSQ)]	C_6H_6	2021, 1931, 1897	1536
[$Re(CO)_3$(*P*-dppe)(DBSQ)]	C_6H_6	2022, 1931, 1893	1535
[$Re(CO)_3(PCy_3)$(DBSQ)]	C_6H_6	2017, 1924, 1892	1528
[$Re(CO)_3$(THF)(DBSQ)]	THF	2019, 1910, 1902	1527
[$Re(CO)_3$(MeC(O)Ph)(DBSQ)]	C_6H_6	2018, 1912 (sh), 1901	1527
[$Re(CO)_3(NEt_3)$(DBSQ)]	C_6H_6	2018, 1915, 1896	1526
[$Re(CO)_3$(py)(DBSQ)]	C_6H_6	2017, 1915, 1897	1526
[$Re(CO)_3(Me_2CO)$(DBSQ)]	C_6H_6[b]	2018, 1901 (broad)	1521
[$Re(CO)_3(Ph_3PO)$(DBSQ)]	C_6H_6	2014, 1901 (sh), 1896	1516
[$Re(CO)_3(Ph_3PO)$(DBSQ)]	CH_2Cl_2	2012, 1899 (broad)	1516
[$Re(CO)_2(P(OPh)_3)_2$(DBSQ)]	CH_2Cl_2	1959, 1881	1489
[$Re(CO)_2(P(OMe)_3)_2$(DBSQ)][c]	$CHCl_3$	1935, 1878	1468
[$Re(CO)_2(PPh_3)_2$(DBSQ)]	CH_2Cl_2	1918, 1839	1426
[$Re(CO)_2(AsPh_3)_2$(DBSQ)]	CH_2Cl_2	1914, 1836	1420
[$Re(CO)_4$(bpy)]$^+$ [d]	nujol	2127, 2030, 1999, 1945	1658
[$Re(CO)_4$(dmb)]$^+$ [d]	nujol	2099, 1982, 1956, 1922	1601
[$Re(CO)_3$(4,4′-bpy)$_2$Cl][e]	CH_2Cl_2	2027, 1926, 1891	1534
[$Re(CO)_3$(bpy)Cl][f]	CH_2Cl_2	2024, 1921, 1899	1534
[$Re(CO)_3(PPh_3)$(bpy)]$^+$ [g]	THF	2037, 1950, 1922	1568
[$Re(CO)_3(PPh_3)$(bpy$^-$)][g]	THF	2015, 1919, 1892	1524
[$Re(CO)_2(PPh_3)_2$(bpy)]$^+$ [h]	CH_2Cl_2	1966, 1894	1505
[$Mn(CO)_4$(DBSQ)]	CH_2Cl_2	2105, 2029, 2004, 1960	1656
[$Mn(CO)_3(PPh_3)$(DBSQ)]	CH_2Cl_2	2024, 1946, 1912	1553
[$Mn(CO)_3(PPh_3)$(DBSQ)]	THF	2025, 1945, 1916	1555
[$Mn(CO)_3$(THF)(DBSQ)]	THF	2029, 1932, 1925 (sh)	1555
[$Mn(CO)_3(H_2O)$(DBSQ)][i]	CH_2Cl_2	2029, 1925 (broad)	1552
[$Mn(CO)_3$(py)(DBSQ)]	py	2026, 1934, 1916	1550
[$Mn(CO)_2(P(OPh)_3)_2$(DBSQ)]	CH_2Cl_2	1968, 1894	1506
[$Mn(CO)_2(P(OPh)_3)_2$(DBSQ)]	THF	1969, 1898	1510
[$Mn(CO)_2(P(OEt)_3)_2$(DBSQ)]	CH_2Cl_2	1946, 1869	1470
[$Mn(CO)_2(P(OEt)_3)_2$(DBSQ)]	THF	1950, 1877	1479
[$Mn(CO)_2(PPh_3)_2$(DBSQ)]	CH_2Cl_2	1927, 1850	1441
[$Mn(CO)_2(PPh_3)_2$(DBSQ)]	THF	1935, 1859	1454
[$Mn(CO)_2(PEt_3)_2$(DBSQ)]	THF	1918, 1849	1433
fac-[$Mn(CO)_3$(bpy)Cl][j]	THF	2025, 1936, 1913	1549
fac-[$Mn(CO)_3(P(OPh)_3)_2$Br][k]	*k*	2053, 2000, 1949	1617
fac-[$Mn(CO)_3(P(OBu)_3)_2$Br][k]	*k*	2037, 1969, 1927	1580
fac-[$Mn(CO)_3(PBu_3)_2$Br][k]	*k*	2008, 1938, 1894	1531
fac-[$Mn(CO)_3(CH_3CN)_3$]$^+$ [l]	CH_3CN	2063, 1974	1622
fac-[$Mn(CO)_3$(py)$_3$]$^+$ [l]	CH_3CN	2041, 1947	1581
fac-[$Mn(CO)_3(Me_2CO)_3$]$^+$ [l]	Me_2CO	2021, 1931	1554

[a] Compounds are listed in the order of decreasing average C≡O force constant, k_{av}. [b] 1:2 (v/v) C_6H_6:Me_2CO mixture. [c] From ref 24. [d] From Shaver, R. J.; Rillema, D. P. *Inorg. Chem.* **1992**, *31*, 4101. bpy = 2,2′-bipyridine, dmb = 4,4-dimethylbipyridine. [e] From ref 58. [f] From George, M. W.; Johnson, F. P. A.; Westwell, J. R.; Hodges, P. M.; Turner, J. J. *J. Chem. Soc., Dalton Trans.* **1993**, 2977 [g] From ref 68. [h] From Caspar, J. V.; Sullivan, B. P.; Meyer, T. J. *Inorg. Chem.* **1984**, *23*, 2104. [i] At 223 K, from ref 31. [j] From Stor, G. J.; Morrison, S. L.; Stufkens, D. J.; Oskam, A. *Organometallics* **1994**, *13*, 2641. [k] From ref 39 and Angelici, R. J.; Basolo, F.; Poë, A. *J. Am. Chem. Soc.* **1963**, *85*, 2215. [l] From Drew, D.; Darensbourg, D. J.; Darensbourg, M. Y. *Inorg. Chem.* **1975**, *14*, 1579. Low-frequency band corresponds to the E-mode in C_{3v} symmetry, measured in $CHCl_2CHCl_2$.

Hyperfine splitting due to the metal nuclei M = ^{55}Mn ($I = 5/2$, 100%), ^{185}Re ($I = 5/2$, 37.1%), and ^{187}Re ($I = 5/2$, 62.9%) and from the donor atoms of the ligand L (^{14}N ($I = 1$, 99.64%), ^{31}P ($I = 1/2$, 100%), ^{121}Sb ($I = 5/2$, 57.25%), ^{123}Sb ($I = 7/2$, 42.75%), and ^{75}As ($I = 3/2$, 100%)) was observed. EPR splitting

(35) Cagné, R. R.; Koval, C. A.; Lisensky, G. C. *Inorg. Chem.* **1980**, *19*, 2854.
(36) Nakamoto, K. *Infrared and Raman Spectra of Inorganic and Coordination Compounds*, 4th ed.; Wiley-Interscience: New York, 1986.
(37) Braterman, P. S. *Metal Carbonyl Spectra*; Academic Press: London, 1975.
(38) Cotton, F. A.; Kraihanzel, C. S. *J. Am. Chem. Soc.* **1962**, *84*, 4432.
(39) Cotton, F. A. *Inorg. Chem.* **1964**, *3*, 702.
(40) Carrington, A.; McLachlan, A. D. *Introduction to Magnetic Resonance*; Chapman and Hall: London, 1979.
(41) Kaim, W. *J. Coord. Chem. Rev.* **1987**, *76*, 187.

Table 2. EPR Parameters of the Re and Mn Carbonyl−Semiquinone Complexes[a]

complex	solvent	g	a_M	a_H	a_L
$[Re(CO)_3(THF)(DBSQ)]$	THF	2.0043	≅7.0		
$[Re(CO)_3(Ph_3PO)(DBSQ)]$	C_6H_6	2.0045	≅8.0		
$[Re(CO)_3(Me_2CO)(DBSQ)]$	C_6H_6[b]	2.0046	11.1		
$[Re(CO)_3(py)(DBSQ)]$	C_6H_6[c]	2.0038	20.1		
$[Re(CO)_3(NEt_3)(DBSQ)]$	C_6H_6	2.0024	24.6		
$[Re(CO)_4(DBSQ)]$	CH_2Cl_2	2.0022	28.2	3.5	
$[Re(CO)_3(AsPh_3)(DBSQ)]$	C_6H_6	2.0010	33.0		33.0
$[Re(CO)_3(AsPh_3)(DBSQ)]$	CH_2Cl_2	2.0006	34.9	3.0	35.7
$[Re(CO)_3(P(OPh)_3)(DBSQ)]$	C_6H_6[d]	2.0013	34.4		30.5
$[Re(CO)_3(P(OPh)_3)(DBSQ)]$	CH_2Cl_2	2.0012	33.6		33.3
$[Re(CO)_3(P(OMe)_3)(DBSQ)]$[e]	C_6H_6	2.0020	35.1		29.2
$[Re(CO)_3(SbPh_3)(DBSQ)]$	C_6H_6	2.0037	37.5		93.7 (^{121}Sb)
					51.0 (^{123}Sb)
$[Re(CO)_3(dppe\text{-}p)(DBSQ)]$	C_6H_6	2.0009	37.6		25.0
$[Re(CO)_3(PPh_3)(DBSQ)]$	C_6H_6	2.0006	38.2		25.0
$[Re(CO)_3(PPh_2Et)(DBSQ)]$	C_6H_6	2.0006	39.0		26.0
$[Re(CO)_3(PBu_3)(DBSQ)]$	C_6H_6	2.0023[f]	40.4		26.9
$[Re(CO)_3(PCy_3)(DBSQ)]$	C_6H_6	2.0016	40.9		23.3
$[Re(CO)_2(P(OPH)_3)_2(DBSQ)]$	CH_2Cl_2	1.9995	42.0		33.3
$[Re(CO)_2(AsPh_3)_2(DBSQ)]$	CH_2Cl_2	1.9956	52.3		35.0
$[Re(CO)_2(PPh_3)_2(DBSQ)]$	CH_2Cl_2	1.9962	59.8		29.4
$[Mn(CO)_3(THF)(DBSQ)]$	THF	2.0044	3.7	3.5[g]	
$[Mn(CO)_3(py)(DBSQ)]$	py	2.0041	6.1	3.2	2.0
$[Mn(CO)_4(DBSQ)]$[h]	CH_2Cl_2	2.0033	7.1	3.35	
$[Mn(CO)_3(H_2O)(DBSQ)]$[i]	CH_2Cl_2	2.0045	7.1	5.6	2.8
$[Mn(CO)_3(PPh_3)(DBSQ)]$	THF[e]	2.0029	9.9	3.3	33.6
$[Mn(CO)_3(PPh_3)(DBSQ)]$	CH_2Cl_2	2.0029	9.9	3.2	34.4
$[Mn(CO)_2(P(OPh)_3)_2(DBSQ)]$	THF	2.0034	11.5	2.8	44.5
$[Mn(CO)_2(P(OEt)_3)_2(DBSQ)]$	THF	2.0039	16.0	2.6	51.0
$[Mn(CO)_2(PPh_3)_2(DBSQ)]$	THF	2.0022	18.3	3.0	42.1
$[Mn(CO)_2(PPh_3)_2(DBSQ)]$	CH_2Cl_2	2.0022	17.9	3.2	39.4
$[Mn(CO)_2(PEt_3)_2(DBSQ)]$	THF	2.0047	28.0		49.5

[a] Compounds are listed in the order of increasing metal hyperfine splitting constant a_M. Splitting constants in Gauss = 0.1 mT. [b] 1:4 (v/v) C_6H_6:Me_2CO mixture. [c] 1:4 (v/v) C_6H_6:py mixture. [d] 1:4 (v/v) $P(OPh)_3$:C_6H_6 mixture. [e] From ref 21. [f] g value from ref 22. [g] Hyperfine splitting due to the 5-Bu^t protons = 0.26 G. [h] From ref 31. [i] Measured at 230 K, from ref 31; a_L corresponds to H_2O protons.

patterns of $[M(CO)_2(L)_2(DBSQ)]$ show that the two ligands L are equivalent in agreement with the *cis*,*trans* configuration. The hyperfine splitting from the $^1H(I = {}^1/_2)$ nucleus of the H atom bound at the C4 position[4] of the DBSQ ligand was observed only for Mn complexes and $[Re(CO)_4(DBSQ)]$. The a_H values are close to that of free DBSQ (3.2 G),[23] consistent with the predominant localization of the unpaired electron on the DBSQ ligand. In other cases, the ^1H splitting was not resolved because of relatively large line widths (1.5−1.8 G for Mn and 7.5−8 G for Re). For the same reason, no ^{14}N hyperfine coupling was found for $[Re(CO)_3(py)(DBSQ)]$ and $[Re(CO)_3(NEt_3)(DBSQ)]$.

Magnitudes of the metal splitting constants show that the spin density on the metal atom is, in all complexes studied, rather small. Thus, the a_M values are comparable with those of "spin-adducts" of $Mn(CO)_5^\bullet$ and $Re(CO)_5^\bullet$ radicals with nitroso compounds[42,43] which were formulated as Mn^I and Re^I complexes of radical-anionic ligands. The a_{Mn} values are much smaller than those observed for a related Mn^0 complex $[Mn(CO)_3(DBCat)]^{2-}$, 53.4 G,[28] and for Mn^{II} complexes.[44] The ratio between a_M and the theoretical splitting constant A_{iso}, calculated[44,45] for an unpaired electron localized in the outer

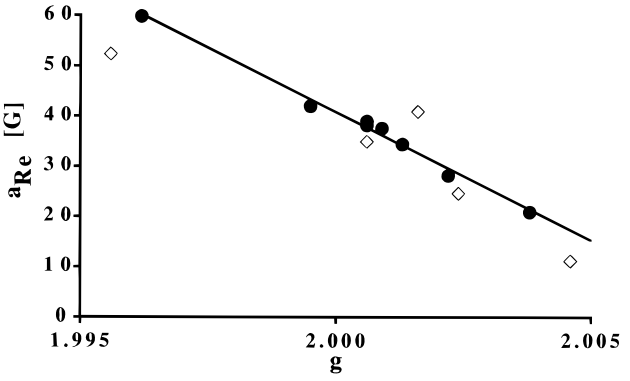

Figure 2. Correlation between the Re hyperfine splitting constants, a_{Re}, and g-factors of the $[Re(CO)_{4-n}(L)_n(DBSQ)]$ complexes. The linear correlation ($R = 0.996$) is based on the data measured for following co-ligands L (●, from left to right): $n = 2$, PPh_3, $P(OPh)_3$; $n = 1$, PPh_2Et, PPh_3, dppe-*p*, $P(OPh)_3$, CO, py. Data for $n = 2$ (L = $AsPh_3$) and for $n = 1$ (L = $AsPh_3$, PCy_3, NEt_3, Me_2CO) (◇, from left to right) are slightly off the line but follow an identical trend.

metal s orbital, ranges from 0.2% to 1.8% for Re−semiquinones and from 0.3% to 2.6% for Mn. Similar low a_M/A_{iso} values were reported[46−49] for complexes of diimine radical-anions bound to metal atoms with a spin-paired d^6 configuration, *e.g.* Cr^0, Mo^0, W^0, Mn^I, and Re^I. From the data in Table 2, it follows that the a_M splitting constants increase with decreasing number of the CO ligands and, for P ligands, in the order $P(OPh)_3$ < $P(OMe)_3$ < PPh_3 < PPh_2Et < PR_3 that reflects their decreasing π-acceptor and increasing σ-donor ability. Increasing electron density on the Re atom raises the energy of the M d(π) orbital, whose interaction with the DBSQ-localized SOMO strengthens. Hence, the changes of a_M splitting constant may be correlated with the changes of the metal-localized spin density transmitted through the d(π)−π* (SOMO) delocalization. This conclusion is fully supported[44] by the observed linear correlation between a_{Re} and the g-factor shown in Figure 2, since the increasing participation of the d(π) orbital in SOMO also increases the contribution from the large spin−orbit coupling of the Re atom, thus diminishing the *g*-factor. Small deviations from the $a_{Re}-g$ correlation observed for complexes with co-ligands like $AsPh_3$, $SbPh_3$, and bulky PCy_3 or hard N and O donors probably reflect[44,45] variations in the radial wave functions of the Re s and d orbitals caused by changes in the Re−L σ-bonding, instead of a different extent of the Re−DBSQ π-bonding.

Rather large a_L values are fully consistent[41] with the ligand L occupying the axial, *i.e. cis*, position with respect to the DBSQ radical ligand. The hyperfine coupling to the co-ligand donor atom originates mainly in the π^*/σ_{ML} hyperconjugation[41,44−47] that is efficient only when the co-ligand is in a position *cis* to the radical ligand with the M−L bond(s) perpendicular to the DBSQ plane. Accordingly, the a_L values observed are rather large, especially in comparison with pseudotetrahedral $[Cu^I(L)_2(DBSQ)]$ complexes[12] where the M−L bonds are bent away from the DBSQ ligand. In addition to the π^*/σ_{ML} mechanism, some spin density is also transmitted to the P atom from the DBSQ ligand through the metal d(π) orbital as is indicated by a_P values found for phosphites (stronger π-acceptors) which are somewhat larger than those for phosphines.

Electronic Absorption Spectra. All the Re−semiquinone complexes studied exhibit a single broad absorption band in

(42) Hudson, A.; Lappert, M. F.; Nicholson, B. K. *J. Chem. Soc., Dalton Trans.* **1977**, 551.
(43) Rehorek, D.; DiMartino, S.; Kemp, T. J. *Z. Chem.* **1989**, *29*, 148.
(44) Goodman, B. A.; Raynor, J. B. *Adv. Inorg. Chem. Radiochem.* **1970**, *13*, 135.
(45) Symons, M. *Chemical and Biological Aspects of Electron-Spin Resonance Spectroscopy*; Van Nostrand Reinhold: Wockingham, England, 1978.
(46) Gross, R.; Kaim, W. *Inorg. Chem.* **1986**, *25*, 498.
(47) Kaim, W.; Kohlmann, S. *Inorg. Chem.* **1990**, *29*, 2909.
(48) Kaim, W. *Inorg. Chem.* **1984**, *23*, 3365.
(49) Kaim, W. *J. Organomet. Chem.* **1984**, *262*, 171.

Table 3. Electronic Absorption Spectra of the Re and Mn Carbonyl−Semiquinone Complexes[a]

complex	solvent	ν_{max}, cm^{-1} (ϵ, M^{-1} cm^{-1})
$[Re(CO)_4(DBSQ)]$	CH_2Cl_2	20240 (5600)
$[Re(CO)_4(DBSQ)]$	C_6H_6	19760 (5500)
$[Re(CO)_3(P(OPh)_3)(DBSQ)]$	C_6H_6[b]	18250 (5300)
$[Re(CO)_3(P(OPh)_3)(DBSQ)]$	CH_2Cl_2	18530 (5300)
$[Re(CO)_3(Me_2CO)(DBSQ)]$	Me_2CO[c]	17990 (4950)
$[Re(CO)_3(Me_2CO)(DBSQ)]$	Me_2CO[d]	17860
$[Re(CO)_3(PPh_3)(DBSQ)]$	C_6H_6	17300 (5800)
$[Re(CO)_3(PPh_3)(DBSQ)]$	CH_2Cl_2	17790
$[Re(CO)_3(PPh_3)(DBSQ)]$	THF	17610
$[Re(CO)_3(AsPh_3)(DBSQ)]$	C_6H_6	17420 (5200)
$[Re(CO)_3(AsPh_3)(DBSQ)]$	CH_2Cl_2	17750 (6300)
$[Re(CO)_3(AsPh_3)(DBSQ)]$	THF	17580
$[Re(CO)_3(THF)(DBSQ)]$	THF[e]	17180 (5350)
$[Re(CO)_3(PPh_2Et)(DBSQ)]$	C_6H_6	17180 (5700)
$[Re(CO)_3(dppe\text{-}p)(DBSQ)]$	C_6H_6	17180 (5700)
$[Re(CO)_3(py)(DBSQ)]$	py[f]	17070 (4800)
$[Re(CO)_3(py)(DBSQ)]$	C_6H_6[g]	16780
$[Re(CO)_3(Ph_3PO)(DBSQ)]$	C_6H_6	16950 (4350)
$[Re(CO)_3(SbPh_3)(DBSQ)]$	C_6H_6	16890 (6050)
$[Re(CO)_3(NEt_3)(DBSQ)]$	C_6H_6	16670
$[Re(CO)_3(PCy_3)(DBSQ)]$	C_6H_6	15970 (5350)
$[Re(CO)_2(P(OPh)_3)_2(DBSQ)]$	CH_2Cl_2	16890 (5500)
$[Re(CO)_2(PPh_3)_2(DBSQ)]$	CH_2Cl_2	14250 (5300), 15870 (sh)
$[Re(CO)_2(AsPh_3)_2(DBSQ)]$	CH_2Cl_2	13920
$[Re(CO)_2(AsPh_3)_2(DBSQ)]$	THF	13700
$[Mn(CO)_4(DBSQ)]$	CH_2Cl_2	19610 (sh), 18480 (2000)
$[Mn(CO)_3(py)(DBSQ)]$	py	19760 (1060), 15240 (2050)
$[Mn(CO)_3(H_2O)(DBSQ)]$[h]	CH_2Cl_2	19230 (2700), 14430 (1500)
$[Mn(CO)_3(THF)(DBSQ)]$	THF	19080 (2370), 14120 (1650)
$[Mn(CO)_3(PPh_3)(DBSQ)]$[h]	CH_2Cl_2	17240 (sh), 15040 (5400)
$[Mn(CO)_2(P(OPh)_3)_2(DBSQ)]$	THF	13550
$[Mn(CO)_2(P(OEt)_3)_2(DBSQ)]$	CH_2Cl_2	12200 (3700)
$[Mn(CO)_2(PPh_3)_2(DBSQ)]$	THF	15290 (1900), 11710 (3900)
$[Mn(CO)_2(PEt_3)_2(DBSQ)]$	THF	<11110

[a] Compounds are listed in the order of decreasing energy of the visible absorption band. [b] 1:4 (v/v) C_6H_6:$P(OPh)_3$. [c] 1:4 (v:v) C_6H_6:Me_2CO. [d] 1:2 (v:v) C_6H_6:Me_2CO. [e] 1:6 (v/v) C_6H_6:THF. [f] 1:4 (v/v) C_6H_6:py. [g] 5:1 (v/v) C_6H_6:py. [h] From ref 31, at 228 K.

the visible spectral region (ϵ = 4300−6500 M^{-1} cm^{-1}) with a long weak ($\epsilon \leq$ 500 M^{-1} cm^{-1}) tail extending into the near infrared spectral region. For $[Re(CO)_4(DBSQ)]$, shoulders were detected at 825 and 980 nm. Band parameters are listed in Table 3.

The maximum of the visible absorption band of $[Re(CO)_{4-n}(L)_n(DBSQ)]$ shifts to lower energies with a decreasing number of CO ligands. Among both the tri- and dicarbonyl series, the absorption energy decreases with decreasing π-acceptor and increasing σ-donor strength of the co-ligand(s) L, *i.e.* with increasing electron density on the Re atom. This co-ligand effect points to the $d(\pi) \rightarrow \pi^*$ (DBSQ) MLCT character of the electronic transition(s) involved. The absorption maxima shift slightly to lower energies with decreasing solvent polarity, in agreement with their MLCT assignment. The $d(\pi) \rightarrow \pi^*$-(DBSQ) transitions are directed into the $3b_1$ SOMO[10,50] of the DBSQ ligand (b_1 refers to the idealized C_{2v} local ligand point group). The $3b_1$ SOMO overlaps with the d_{yz} metal orbital (see Figure 1 for axes orientation). Therefore, the $d_{yz} \rightarrow 3b_1$ transition is expected to be the most intense of the three $d(\pi) \rightarrow 3b_1$ MLCT transitions possible and, hence, responsible for the main visible absorption band. This assignment is also in line with earlier[6,9,10,51,52] studies on electronic spectra of other semiquinone complexes. Further weak transitions that might contribute to the absorption band and to its low-energy tail may belong either to the less intense $d_{x^2-z^2} \rightarrow 3b_1$ and $d_{xz} \rightarrow 3b_1$ MLCT or to the DBSQ-localized intraligand transitions. The latter have been observed to occur below 15 000 cm^{-1} with extinction coefficients lower than 500 M^{-1} cm^{-1} for free DBSQ[53] as well as for many of its complexes.[10,51] These intraligand transitions were described[10,51] as $n \rightarrow \pi^*(3b_1 -$ SOMO), the n orbital being the symmetrical ($9a_1$) combination of the lone electron pairs of the two DBSQ oxygen donor atoms. This assignment was based on CNDO/2 and Fenske−Hall calculations[10,50] of the 1,2-benzosemiquinone molecule which indicated that the n($9a_1$) orbital is the HOMO of the free ligand. However, these calculations take into account neither the ligand open-shell nature nor the strong involvement of the $9a_1$ orbital in the σ-bonding to the metal. Therefore, we expect the n($9a_1$) $\rightarrow \pi^*(3b_1)$ transition to occur at higher energies and to be rather dependent on the nature of the metal atom. Hence, we prefer to assign the weak low-energy absorption to π^*(SOMO) $\rightarrow \pi^{**}$ transitions of the DBSQ ligand. Analogous transitions were found in many other organic radical-anions.[54,55]

Spectra of the Mn complexes usually show two broad bands in the visible region tailing into NIR. One band with a shoulder on its high-energy side was found[31] for $[Mn(CO)_4(DBSQ)]$, $[Mn(CO)_3(PPh_3)(DBSQ)]$, and $[Mn(CO)_2(PPh_3)_2(DBSQ)]$. Their extinction coefficients are lower than those for Re. Except for $[Mn(CO)_3(H_2O)(DBSQ)]$ and $[Mn(CO)_3(THF)(DBSQ)]$, the main absorption band shifts to lower energy with increasing σ-donor and decreasing π-acceptor properties of the co-ligand-(s). This trend is most obvious in the $[Mn(CO)_2(L)_2(DBSQ)]$ series and supports the assignment of the main absorption maximum to the $d_{yz} \rightarrow 3b_1$ MLCT transition. The less intense absorption band present in the spectra of some of the Mn^I complexes studied, see Table 3, may be assigned to other $d(\pi) \rightarrow 3b_1$ MLCT transition(s). Intraligand DBSQ-localized transitions contribute again to the low-energy weak absorption that extends into the NIR.

All the Re− and Mn−semiquinone complexes have very strong absorptions in the UV region which belong to the DBSQ intraligand transitions. This is manifested by the narrow band at 310 nm (ϵ = 9380 M^{-1} cm^{-1}) for $[Mn(CO)_3(THF)(DBSQ)]$ which is very similar to the absorption band[53] of free DBSQ. Analogously, both $[Re(CO)_4(DBSQ)]$ and $[Re(CO)_3(PPh_3)-(DBSQ)]$ show a band at 282 nm, $\epsilon \simeq 10^4$ M^{-1} cm^{-1}. The spectral transitions in the UV region were not studied further.

Resonance Raman Spectra. Resonance Raman (rR) spectra of $[Re(CO)_4(DBSQ)]$, $[Re(CO)_3(PPh_3)(DBSQ)]$, and $[Re(CO)_2-(PPh_3)_2(DBSQ)]$ are shown in Figure 3, and selected data are presented in Table 5. Intensities of all the Raman bands decrease when the excitation was tuned to shorter wavelengths, out of the visible absorption band, thus proving their (pre)-resonance intensity enhancement. The rR spectra are dominated by a strong peak in the 1400−1450 cm^{-1} range, *i.e.* in the region characteristic[2,3,6,11] of the ν(C═O) stretching vibration of coordinated semiquinones. Raman bands at 1524 and 1528 cm^{-1} found for $[Re(CO)_4(DBSQ)]$ and $[Re(CO)_3(PPh_3)-(DBSQ)]$, respectively, as well as a group of weaker bands between 1240 and 1400 cm^{-1} may be assigned to the intraligand C−C vibrations. Raman band due to the highest-frequency A_1

(50) Gordon, D. J.; Fenske, R. F. *Inorg. Chem.* **1982**, *21*, 2907.
(51) Dodsworth, E. S.; Lever, A. B. P. *Chem. Phys. Lett.* **1990**, *172*, 151.
(52) Dei, A.; Pardi, L. *Inorg. Chim. Acta* **1991**, *181*, 3.
(53) Stallings, M. D.; Morrison, M. M.; Sawyer, D. T. *Inorg. Chem.* **1981**, *20*, 2655.
(54) Krejčík, M.; Záliš, S.; Ladwig, M.; Matheis, W.; Kaim, W. *J. Chem. Soc., Perkin Trans. 2* **1992**, 2007.
(55) Photostability of the Re complexes might be used as an argument against a contribution from the $n \rightarrow \pi^*$ intraligand transition to the visible absorption band. Such a transition would be expected to strongly labilize the M−DBSQ bonding. The same is true for a weak (π^*-SOMO) $3b_1 \rightarrow$ M LMCT transition which could also occur in the visible region.

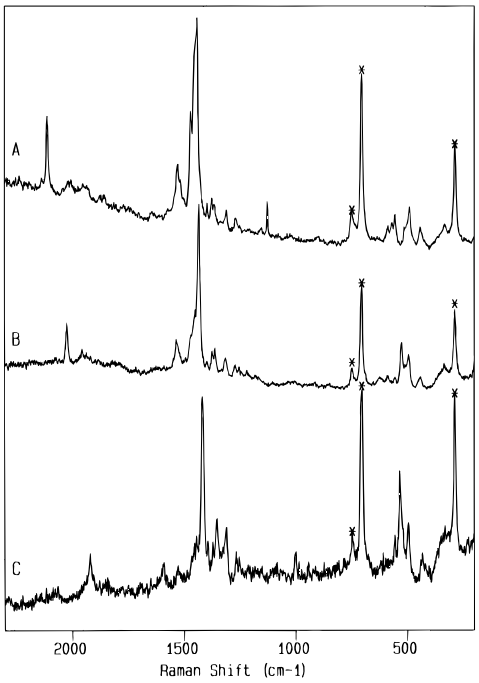

Figure 3. Resonance Raman spectra of $[Re(CO)_4(DBSQ)]$ (A) $[Re(CO)_3(PPh_3)(DBSQ)]$ (B), and $[Re(CO)_2(PPh_3)_2(DBSQ)]$ (C). Excitation wavelengths: 514.5, 579, and 621 nm, respectively. An asterisk (*) denotes Raman peaks of the CH_2Cl_2 solvent.

ν(C≡O) mode occurs at 2111, 2023, and 1919 cm^{-1} for the tetra-, tri-, and dicarbonyls, respectively. Another important group of three Raman peaks occurs in the range 480−550 cm^{-1}. By analogy with five-membered chelate rings involving oxygen donor atoms, *e.g.* oxalates, and with $[Ru(bpy)_2(SQ)]^+$, these peaks may be assigned[36,56,57] to skeletal vibrations of the Re(DBSQ) chelate ring. The central most prominent peak of $[Re(CO)_3(PPh_3)(DBSQ)]$ and $[Re(CO)_2(PPh_3)_2(DBSQ)]$ probably corresponds to the symmetrical Re−O stretching vibration that is partly coupled to the C_1-C_2 stretch,[36,56,57] ν(Re−O). For $[Re(CO)_4(DBSQ)]$, this group of peaks looks like one peak at 492 cm^{-1} with two shoulders at 502 and 510 cm^{-1}. We tentatively assign the central shoulder at 502 cm^{-1} to ν(Re−O). (Alternative ν(Re−O) assignment to the main peak at 492 cm^{-1} is less probable as this band is exhibited by all three complexes.) Other weak Raman peaks observed at frequencies below 700 cm^{-1} correspond to bending vibrations of the Re(DBSQ) ring, δ(M-C≡O), and ν(M−C) vibrations.[36,56,57]

The enhancement of the Raman bands due to the intra-DBSQ ν(C═O) and ν(C≡O) vibration is in full agreement[58−60] with the d(π) → $3b_1$ MLCT character of the resonant electronic transition which affects the DBSQ C═O bonds through the population of the C═O π-antibonding[10,51] $3b_1$ orbital. The C−C bonds are affected to a much lesser extent as $3b_1$ is only weakly antibonding to the C(3)−C(4) and C(5)−C(6) bonds and weakly bonding with respect to the C(1)−C(2) and C(2)−C(3), C(4)−C(5), and C(6)−C(1) bonds.[10,50] Hence, the peaks due to C−C vibrations exhibit much smaller enhancement. The Raman peak due to the ν(C≡O) vibration is enhanced because of the depopulation of the d(π) orbital(s), involved in the Re→CO back-bonding, upon the MLCT excitation.[58]

Observation of the resonant enhancement of the ν(Re−O) peak shows that the bonding within the Re(DBSQ) chelate ring is also affected by the MLCT excitation. Generally, we may expect[59,60] that the enhancement of this peak will increase with increasing mixing between the d_{yz} and $3b_1$ orbitals, which is equivalent to a partial π-bonding between Re and DBSQ. The MLCT excitation then gains, in part, a character of a π(Re−O) → π^*(Re−O) transition. The effect of the electronic excitation on the Re−O and semiquinone C═O bonds may be compared using the ratio between the intensities of the Raman bands due to corresponding stretching vibrations. It may be approximately expressed as[61]

$$\frac{I_a}{I_b} = \frac{\omega_a^2 \Delta_a^2}{\omega_b^2 \Delta_b^2} \qquad (1)$$

where ω is the vibration frequency and Δ is the displacement of corresponding normal coordinates upon the resonant electronic excitation. Calculated Δ(Re−O)/Δ(C═O) ratios of the ν(Re−O) and ν(C═O) normal mode displacements, shown in Table 5, indicate rather strong relative excited state distortion of the skeletal normal modes of the Re(DBSQ) ring which increases with decreasing number of CO ligands.

Table 4. Oxidation and Reduction Potentials (V *vs* Fc/Fc^+) of the Re and Mn Carbonyl−Semiquinone Complexes[a]

complex	solvent	$E_{1/2}$(ox)	$E_{1/2}$(red)	$\Delta E_{1/2}$[b]
$[Re(CO)_4(DBSQ)]$	CH_2Cl_2[c]	+0.43	−0.51[d]	0.94
$[Re(CO)_3(THF)(DBSQ)]$	THF	+0.41	−0.63	1.04
$[Re(CO)_3(PCy_3)(DBSQ)]$	CH_2Cl_2	+0.37[e]	−0.85	
$[Re(CO)_3(P(OPh)_3)(DBSQ)]$	CH_2Cl_2[c]	+0.36	−0.67[d]	1.03
$[Re(CO)_3(Me_2CO)(DBSQ)]$	CH_2Cl_2[c]	+0.36	−0.52	0.88
$[Re(CO)_3(py)(DBSQ)]$	CH_2Cl_2	+0.35[f]	−0.71	1.06
$[Re(CO)_3(NEt_3)(DBSQ)]$	CH_2Cl_2	+0.32	−0.65	0.97
$[Re(CO)_3(Ph_3PO)(DBSQ)]$	CH_2Cl_2	+0.30	−0.66[d]	0.96
$[Re(CO)_3(SbPh_3)(DBSQ)]$	CH_2Cl_2	+0.29	−0.62	0.91
$[Re(CO)_3(AsPh_3)(DBSQ)]$	CH_2Cl_2	+0.28	−0.70[d]	0.98
$[Re(CO)_3(PPh_3)(DBSQ)]$	CH_2Cl_2	+0.24	−0.87	1.11
$[Re(CO)_3(dppe\text{-}p)(DBSQ)]$	CH_2Cl_2	+0.23[f]	−0.85	1.08
$[Re(CO)_3(PPh_2Et)(DBSQ)]$	CH_2Cl_2	+0.20[f]	−0.85	1.05
$[Re(CO)_2(P(OPh)_3)_2(DBSQ)]$	CH_2Cl_2	+0.14	−0.92[f]	1.06
$[Re(CO)_2(AsPh_3)_2(DBSQ)]$	CH_2Cl_2	−0.15	−1.04[d]	0.89
$[Re(CO)_2(PPh_3)_2(DBSQ)]$	CH_2Cl_2	−0.21	−1.14	0.93
$[Mn(CO)_4(DBSQ)]$	CH_2Cl_2	+0.29	−0.80[d,f]	
$[Mn(CO)_3(THF)(DBSQ)]$	THF	+0.23	−0.70	0.93
$[Mn(CO)_3(py)(DBSQ)]$	py	+0.11[d,f]	−0.90	
$[Mn(CO)_3(PPh_3)(DBSQ)]$	CH_2Cl_2	+0.04	−0.92	0.96
$[Mn(CO)_2(P(OEt)_3)_2(DBSQ)]$	CH_2Cl_2	−0.37	−1.25[g]	0.88
$[Mn(CO)_2(P(OEt)_3)_2(DBSQ)]$	THF	−0.27	−1.25	0.98
$[Mn(CO)_2(PEt_3)_2(DBSQ)]$	THF	−0.42	−1.39[h]	0.97
$[Mn(CO)_2(PPh_3)_2(DBSQ)]$	CH_2Cl_2	−0.46	−1.26[d,f]	
uncoordinated DBSQ	THF	−1.09	−1.70	0.61

[a] For composition of the solutions, see Table 3. 10^{-1} M Bu_4NPF_6 added. Scan rate: 100 mV/s. Compounds are listed in the order of decreasing oxidation potential. [b] $\Delta E_{1/2} = E_{1/2}(ox) - E_{1/2}(red)$. [c] At 203 K. [d] Electrochemically irreversible, ΔE_p > 100 mV. Large ΔE_p (120 − 140 mV at room temperature observed for the reductions of Re complexes (L = CO, Ph_3PO, Me_2CO, $P(OPh_3)$, $AsPh_3$) appears to be caused by subsequent chemical reactions.[31] [e] Complicated oxidation mechanism, electrode passivation. [f] Chemically irreversible (Mn) or partly reversible (Re). [g] In the presence of excess $P(OEt)_3$. [h] In the presence of excess PEt_3.

Electrochemistry. Table 4 summarizes the reduction and oxidation potentials of the complexes investigated. Unless stated otherwise, the redox couples listed in Table 4 are electrochemi-

(56) Fujita, J.; Martell, A. E.; Nakamoto, K. *J. Chem. Phys.* **1962**, *36*, 324, 331.
(57) Stufkens, D. J.; Snoeck, Th. L.; Lever, A. B. P. *Inorg. Chem.* **1988**, *27*, 953.
(58) Gamelin, D. R.; George, M. W.; Glyn, P.; Grevels, F.-W.; Johnson, F. P. A.; Klotzbücher, W.; Morrison, S. L.; Russell, G.; Schaffner, K.; Turner, J. J. *Inorg. Chem.* **1994**, *33*, 3246.
(59) Stufkens, D. J. *Coord. Chem. Rev.* **1990**, *104*, 39 and references therein.
(60) Servaas, P. C.; van Dijk, H. K.; Snoeck, T. L.; Stufkens, D. J.; Oskam, A. *Inorg. Chem.* **1985**, *24*, 4494.
(61) Zink, J. I.; Kim Shin, K.-S. *Adv. Photochem.* **1991**, *16*, 119.

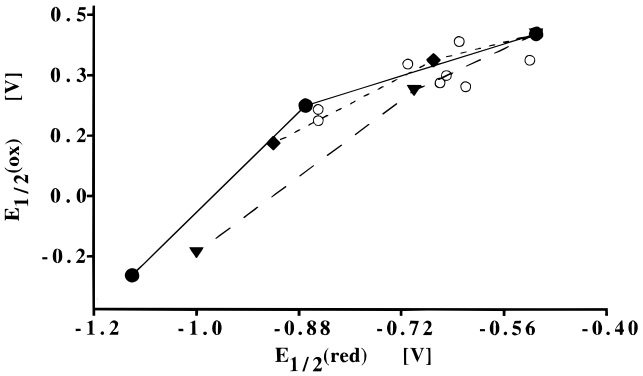

Figure 4. Correlation between the oxidation and reduction potentials of the $[Re(CO)_{4-n}(L)_n(DBSQ)]$ complexes. Members of the $[Re(CO)_{4-n}(PPh_3)_n(DBSQ)]$ series (●) are connected by a full line, members of the $[Re(CO)_{4-n}(P(OPh)_3)_n(DBSQ)]$ series (◆) by a short-dashed (- - -) line, and members of the $[Re(CO)_{4-n}(AsPh_3)_n(DBSQ)]$ series (▼) by a long-dashed line (− − −). Unconnected points (○) correspond to $[Re(CO)_3(L)(DBSQ]$ complexes. From left to right: L = PPh_2Et, dppe-*p*, py, Ph_3PO, NEt_3, THF, $SbPh_3$, Me_2CO.

cally reversible or quasireversible. As we have shown previously,[28−31] both the oxidation and reduction are localized on the DBSQ ligand, producing quinone and catecholate complexes, respectively. Complicated chemistry that follows the reduction of some Re complexes[30] (Table 4, footnote *c*) was suppressed by using low temperatures. Reduction potentials of the Mn complexes were measured in the presence of an excess of free L to minimize the effects of the dissociation of the co-ligand L upon the reduction.[28,29] Even so, related structural change renders the reduction couples quasireversible or, for $[Mn(CO)_4(DBSQ)]$ and $[Mn(CO)_2(PPh_3)_2(DBSQ)]$, even irreversible.

Neglecting the changes in the entropy and solvation energy, and assuming that neither the energies nor the (de)localization of the redox orbitals are dependent on the number of electrons in the molecule, the reduction potential of spin-doublet semiquinone complexes may be expressed[62,63] by the SOMO orbital energy, ϵ_i, and the Coulombic integral J_{ii}: $E_{1/2}(\text{red}) = -\epsilon_i - J_{ii}$ + constant. The oxidation potential is related to ϵ_i only,[62,63] $E_{1/2}(\text{ox}) = -\epsilon_i$ + constant. The difference between the oxidation and reduction potentials ($\Delta E_{1/2}$, Table 4) is then approximately equal to the value of J_{ii} (positive). If both the oxidation and reduction were indeed fully DBSQ-localized, the redox potentials were expected to be nearly independent of the composition of the coordination sphere and $\Delta E_{1/2}$ expected to be constant and close to the free ligand value, 0.61 V. A linear correlation between $E_{1/2}(\text{ox})$ and $E_{1/2}(\text{red})$ would then be predicted. Data in Table 4 clearly show that $\Delta E_{1/2}$ is much larger than expected, around 1 V. The general trend of decreasing oxidation potential with decreasing reduction potential was observed, although the linear correlation predicted by the simple model was not found (see Figure 4). The largest deviations occur for $[Re(CO)_2(L)_2(DBSQ)]$ whose oxidation potentials appear to be smaller than expected. The same effect occurs in the Mn series, see Table 4.

Dependence of the ligand-localized redox potentials on the co-ligands may also be discussed in terms of the ligand-specific electrochemical parameters $E_L(L)$[64,65] whose sum, $\sum E_L(L)$, should correlate linearly with the redox potentials. Reduction potentials of all the $[Re(CO)_{4-n}(L)_n(DBSQ)]$ complexes studied, regardless of the number (n = 0, 1, 2) and nature of the co-ligands L, follow the same linear correlation with the $\sum E_L(L)$ parameter: slope = 0.5, intercept = −2.4 V *vs* Fc/Fc^+. For the oxidation potentials, two distinct correlations were found, one for the $[Re(CO)_4(DBSQ)]$ and $[Re(CO)_3(L)(DBSQ)]$ complexes (slope = 0.3, intercept = −0.7 V) and another for the $[Re(CO)_2(L)_2(DBSQ)]$ species (slope = 0.8, intercept = −2.4 V). Both the much larger slope and much more negative intercept found for the oxidation of the dicarbonyls indicate a much larger influence of the Re−DBDiox electronic coupling on the potential of the $[Re(CO)_2(L)_2(DBQ)]^+/[Re(CO)_2(L)_2(DBSQ)]$ redox couple than on the oxidation of the tri- and tetracarbonyl semiquinones. However, these differences in the electronic delocalization have to be much larger in the oxidized products, $[Re(CO)_{4-n}(L)_n(DBQ)]^+$, than in the parent semiquinones, since the discontinuity between the tri- and dicarbonyls was not found for the reduction potentials.

To account for these observations, it should be noted that both the wave function and energy of the $3b_1$ frontier orbital and, hence, the extent of the metal−dioxolene delocalization depend strongly on the oxidation state of the dioxolene ligand.[11] From the electrochemical data alone, it is thus difficult to distinguish whether the co-ligand dependence of the redox potentials arises from a strong electronic delocalization in the semiquinone complexes themselves or in their redox products, *i.e.* quinone and catecholate complexes. The redox potentials may then be expressed as

$$E_{1/2}(\text{red}) = -\epsilon_i - J_{ii} - E_r(\text{red}) + \text{constant} \qquad (2)$$

$$E_{1/2}(\text{ox}) = -\epsilon_i + E_r(\text{ox}) + \text{constant} \qquad (3)$$

where E_r(red) and E_r(ox) stand for the relaxation energies (negative) which correspond to an extra stabilization of the reduced and oxidized product, respectively, by changes of the orbital and correlation energies upon the electron transfer. For dioxolene complexes, these quantities might be the dominant contributions to the redox potentials. The spectroscopic studies of the Mn^I and Re^I quinone and catecholate complexes suggest that E_r(ox) is the most important term, especially for the $[M(CO)_2(L)_2(DBSQ)]$ which are oxidized to exceptionally stable quinone complexes with a delocalized $M(DBQ)^+$ bonding.[28−31] Consequently, the oxidation potentials of $[Re(CO)_2(PPh_3)_2(DBSQ)]$ and $[Re(CO)_2(AsPh_3)_2(DBSQ)]$, and, to a lesser extent, also of $[Re(CO)_2\{P(OPh)_3\}_2(DBSQ)]$, are more negative than expected either from the general trend between the oxidation and reduction potentials (Figure 4) or from the $\sum E_L(L)$ electrochemical parameters.

Oxidation States and the Co-ligand Effects. Compounds investigated in this study have three electrons in two frontier orbitals, the metal d(π) and dioxolene $3b_1$, whose interaction is symmetry allowed. Therefore, we should distinguish between $[M^I(DBSQ)]$ and $[M^{II}(DBCat)]$ valence isomers characterized by $[(d(\pi))^2(3b_1)^1]$ and $[(3b_1)^2(d(\pi))^1]$ electron configurations, respectively. Alternatively, very strong M → DBSQ π-back-donation could result in a delocalized M(DBDiox) bonding characterized by a $[(d(\pi) + 3b_1)^2(d(\pi) - 3b_1)^1]$ configuration.

The spectroscopic and electrochemical data discussed in the preceding sections provide compelling evidence that all the $[M(CO)_{4-n}(L)_n(DBSQ)]$, n = 0, 1, 2, complexes investigated may best be formulated as containing a radical-anionic DBSQ ligand bound to a formally M^I central atom with a spin-paired d^6 configuration, regardless the number of the CO ligands and the nature of the co-ligand(s) L. This conclusion is also in full agreement with the molecular structure[66] of $[Re(CO)_3(PPh_3)(DBSQ)]$ which meets all the usual structural criteria[2,3,11,67] for a coordinated semiquinone ligand.

(62) Vlček, A. A. *Electrochim. Acta* **1968**, *13*, 1063.
(63) Záliš, S.; Krejčík, M.; Drchal, V.; Vlček, A. A. *Inorg. Chem.* **1995**, *34*, 6008.
(64) Lever, A. B. P. *Inorg. Chem.* **1990**, *29*, 1271.
(65) Dodsworth, E. S.; Vlček, A. A.; Lever, A. B. P. *Inorg. Chem.* **1994**, *33*, 1045.

Table 5. Variation of the Spectral and Electrochemical Properties with the Number of CO Ligands within the $[Re(CO)_{4-n}(PPh_3)_n(DBSQ)]$ Series[a]

	$Re(CO)_4(DBSQ)$	$Re(CO)_3(PPh_3)(DBSQ)$	$Re(CO)_2(PPh_3)_2(DBSQ)$
k_{av}, N m^{-1}	1635	1534	1426
$\tilde{\nu}$(C═O), cm^{-1}	1439	1430	1413
$\tilde{\nu}$(Re−O), cm^{-1}	502	524	532
I(Re−O)/I(C═O)	0.11	0.27	0.53
Δ(Re−O)/Δ(C═O)	1.0	1.4	1.9
a_{Re}, G	28.2	38.2	59.8
a_{Re}/A_{iso}, %	0.9	1.2	1.9
g	2.0022	2.0006	1.9962
E(MLCT), cm^{-1}	20240	17790	14250
$E_{1/2}$(ox), V	+0.43	+0.24	−0.21
$E_{1/2}$(red), V	−0.51	−0.87	−1.14

[a] See text for the explanation of the symbols.

The influence of the nature of the co-ligands on the properties of the $[M(CO)_{4-n}(L)_n(DBSQ)]$, $n = 0, 1, 2$, complexes may be interpreted by competitive M → DBSQ and M → CO π-back-bonding. From this point of view, comparison of the data obtained for the $[Re(CO)_{4-n}(PPh_3)_n(DBSQ)]$ ($n = 0, 1, 2$) series, summarized in Table 5, is especially revealing. Data obtained on other $[M(CO)_{4-n}(L)_n(DBSQ)]$ ($n = 0, 1, 2$; M = Re, Mn) series follow identical trends, see Tables 1−4. Increasing electron donation to the metal atom from the co-ligand(s) L along the $n = 0, 1, 2$ series or by using a more basic L raises the metal d(π) orbital energy. This is manifested by the shift of the Re → DBSQ MLCT absorption band to lower energies. The metal atom becomes a stronger π-donor, and both the M → DBSQ and M → CO π-back-bonding are strengthened. This is accompanied by a large decrease of the average C≡O stretching force constants k_{av}. For example, going from $[Re(CO)_4(DBSQ)]$ to $[Re(CO)_3(PPh_3)(DBSQ)]$, the k_{av} value drops by 101 N m^{-1}. The replacement of another CO ligand in $[Re(CO)_3(PPh_3)(DBSQ)]$ to $[Re(CO)_2(PPh_3)_2(DBSQ)]$ results in the k_{av} decrease by another 108 N m^{-1}. For comparison, the same sequential CO substitutions in the $[Re(CO)_4(bpy)]^+$ complex are accompanied[68] by a k_{av} decrease by 90 and 60 N m^{-1} only, see Table 1, suggesting that the π-acceptor capacity of the DBSQ ligand is significantly smaller than that of 2,2′-bipyridine. IR data thus show that the changes in the electron density on the metal atom induced by the co-ligand(s) are compensated mostly by the π-back-bonding to the CO-ligands.

Nevertheless, the properties of the $[M(CO)_{4-n}(L)_n(DBSQ)]$ complexes studied are strongly influenced by the M → DBSQ π-back-bonding whose extent depends on the co-ligands. This is shown by coherent trends of all relevant parameters listed in Table 5. The decrease of the intra-DBSQ ν(C═O) frequency and of the g factor and parallel increase of the Re hyperfine splitting constant a_{Re} with decreasing number of CO ligands along the $[Re(CO)_{4-n}(L)_n(DBSQ)]$, $n = 0, 1, 2$, series point to an increasing donation of the d(π) electron density from Re to the $3b_1$ (*i.e.* C═O antibonding) orbital. Correlations between these parameters (see Figures 2 and 5) indeed show that they reflect the same structural factor, namely the Re−DBSQ π-delocalization that results from the d(π) − $3b_1$ mixing. Parallel evidence for increasing Re−DBSQ π-interaction along this series is provided by the electronic transition which changes in character along the $[Re(CO)_{4-n}(PPh_3)_n(DBSQ)]$, $n = 0, 1, 2$, series from d(π) → $3b_1$ MLCT to partly delocalized (d(π) + $3b_1$) → (d(π) − $3b_1$). This is manifested by increasing excited state distortion of the bonds involved in the ν(Re−O) vibrational mode relative to the distortion of the DBSQ C═O bonds (see Table 5, Δ(Re−O)/Δ(C═O)). Increasing Re → DBSQ π-back-bonding also results in strengthening of the Re−O bond and, possibly, of the electronic and vibrational coupling within the Re−O−C_1−C_2−O chelate ring, as is shown by increasing ν(Re−O) frequency with decreasing number of CO ligands. The negative shift of redox potentials with increasing electron donation from the co-ligand(s) reflects an increase in the energy of the DBSQ $3b_1$ redox orbital caused by increasing mixing with the metal d(π) orbital. In addition, extra stabilization of $[M(CO)_2(L)_2(DBQ)]^+$ oxidation products[28−31] contributes to the drop in oxidation potentials between tricarbonyls and dicarbonyls. Interestingly, a correlation was found between $E_{1/2}$(ox) and the parameters that reflect the strength of the Re−DBSQ π-interaction, namely a_{Re} and the intra-DBSQ ν(C═O) frequency (see Figure 5). Apparently, the increase of the delocalization energy upon the oxidation depends on the composition of the coordination sphere in the same way as the π-interaction within the Re(DBSQ) chelate ring itself. Interestingly, the sensitivity of the spectroscopic and electrochemical parameters to the co-ligand and even solvent nature is higher in the dicarbonyl than tricarbonyl series, apparently because of lower π-acceptor capacity of the $M(CO)_2$ fragment compared with that of $M(CO)_3$.

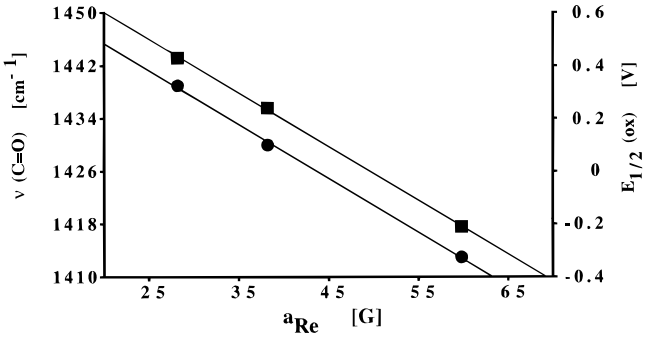

Figure 5. Correlation of the intra-DBSQ ν(C═O) stretching frequency (●) and of the oxidation potential $E_{1/2}$(ox) (■) with the Re hyperfine splitting constants, a_{Re}, in the $[Re(CO)_{4-n}(PPh_3)_n(DBSQ)]$ series.

The spectroscopic and electrochemical data thus provide definite evidence for a limited π-donation from Re^I or Mn^I to the DBSQ ligand whose extent may be finely tuned by the co-ligands. The absolute magnitude of the M → DBSQ π-back-donation remains, however, rather low. Importantly, all the spectroscopic parameters change gradually with changing composition of the coordination sphere, ruling out any switchover to a valence isomer other than $[M^I(DBSQ)]$ within the $[M(CO)_{4-n}(L)_n(DBSQ)]$ ($n = 0, 1, 2$) series, regardless of the nature of the co-ligands. The carbonyl−semiquinone complexes

(66) Cheng, C. P.; Wang, S. R.; Lin, J. C.; Wang, S.-L. *J. Organomet. Chem.* **1988**, *249*, 375.
(67) Carugo, O.; Castellani, C. B.; Djinovic, K.; Rizzi, M. *J. Chem. Soc., Dalton Trans.* **1992**, 837.
(68) Stor, G. J.; Hartl, F.; van Outersterp, J. W. M.; Stufkens, D. J. *Organometallics* **1995**, *14*, 1115.

of Re^{I} and Mn^{I} thus behave differently from some other semiquinone complexes, *e.g.* of Cu or Co, that exhibit a co-ligand-controlled $[Cu^{I})L_2)(DBSQ)]/[Cu^{II}(L_2)(DBCat)]$, $[Mn^{II}(L_2)(DBSQ)_2]/[Mn^{III}(L_2)(DBCat)(DBSQ)]/[Mn^{IV}(L_2)(DBCat)_2]$, or $[Co^{II}(DBSQ)]/[Co^{III}(DBCat)]$ switching.[12−18] Noteworthy, the metal d(σ) and dioxolene $3b_1(\pi^*)$ frontier orbitals of the bistable Cu and Co semiquinone complexes are orthogonal, not interacting with each other. It thus appears that the bistability of the Re^{I}− and Mn^{I}−semiquinones is prevented by the direct π-interaction between the d(π) metal-HOMO and the $3b_1$ DBSQ-SOMO and by the presence of CO ligands which very effectively compensate for the changes in the electron density on the metal atom. Although the M → DBSQ π-bonding becomes more important upon raising the electron density on the metal atom, the CO ligands are far better π-acceptors, thus "shielding" the semiquinone ligand from the metal-localized electronic effects induced by the co-ligands and keeping the d(π) electrons energetically well below the $3b_1$ SOMO of the DBSQ ligand. The amount of electron density transferred from the metal to the semiquinone ligand is then not sufficient to induce the structural changes necessary[11] for a switchover to the $[M^{II}(DBCat)]$ valence isomer.

Acknowledgment. Financial support from the Granting Agency of the Czech Republic (203/93/0250), the Netherlands Foundation for Chemical Research (SON), the Netherlands Organization for the Advancement of Pure Research (NWO), European Research Network, and COST programs are gratefully appreciated.

IC950018O